



EFFECT OF GEOMETRICAL FEATURES ON HYDRODYNAMIC PERFORMANCES OF THE CONTRA-ROTATING PROPELLER

F. Bouregba^{1*}, M. Belkadi¹, M. Aounallah¹ and L. Adjout¹

¹Laboratoire d'Aero-Hydrodynamique navale LAHN, USTO-MB, Oran, Algeria.

*E-mail : fatimabouregba@hotmail.com, fatima.bouregba@univ-usto.dz

Abstract :

New contra-rotating four-bladed DTMB propeller configurations operating in open water are numerically studied to determine their hydrodynamic performances. The unsteady turbulent flow around propellers is modeled by RANS equations with SST $k-\omega$ turbulence model and solved by a CFD software. The computational domain is divided into two blocks linked with a rotating interface. The predicted results show that the thrust and efficiency of the contra-rotating propellers (CRPs) increase compared to the single propeller, leading to a significant reduction of the propeller diameter. The variation in axial spacing and angular displacement seems to have little effect on the CRPs efficiency. The results also show that the thrust can be further improved by adopting a moderate negative twist angle of the rear propeller.

Keywords: Contra-rotating propellers (CRPs), axial spacing, angular spacing, twist angle, CFD.

NOMENCLATURE

D	Propeller diameter	u_i	Time average velocity
J	Advance coefficient	$\overline{u'_i u'_j}$	Reynolds stress
K_Q	Total torque coefficient	Z	Blade number
K_T	Total thrust coefficient	Greek symbols	
L/D	Axial spacing	α	Twist angle
n	Propeller rotational speed	ρ	Water density
P	Time average pressure	μ	Dynamic viscosity
Q	Total torque	η_0	Propeller efficiency
T	Total thrust	θ	Angular displacement
t	Time		

1. Introduction

The performance of marine propellers and in particular their propulsive efficiencies have not ceased to undergo spectacular progress since their invention. Several types of thrusters have been developed such as the contra-rotating propellers which the principle is based on the use of two propellers mounted on two coaxial shafts. The advantages of these propellers include the possibility to recover a part of the forward propeller rotational energy loss which leads to better efficiency and the possibility to use a lower rotational speed for the same diameter compared to a single propeller. Although on commercial vessels mechanical complications and high maintenance costs prevent the adoption of this system, some offshore vessels still use this technology. The application of CRPs to ships allows providing more power on the same engine without fearing the appearance of the cavitation phenomenon. As for its application to torpedoes, the torque compensation generated by the front propeller is insured by the second one, which facilitates the rectilinear trajectories without piloting.

Among all the researchers who contributed to the performance study of contra-rotating propellers, it is obvious to mention first the work of Miller (1976) for his experimental investigation on the CRPs behavior in open water. He observed that for high advance coefficients, the thrust of the front propeller is greater than that of the

rear propeller. Tsakonas et al. (1983) applied the lifting surface theory to predict the hydrodynamic performance of CRP and concluded that CRPs performance can be improved when the blade number of the two propellers is different. Yang et al. (1991) used the same method to predict CRPs performance by taking into account the interactions between the vortices of the two propellers where the wake model of Yang (1990) was applied. The latter was able to predict the rear vortices structure. In the same context, Hoshino (1994) applied the lifting surface theory to predict the thrust of CRPs operating in a straight line, port turn and starboard turn. The results of the models treated are in good agreement with the experimental results. Sasaki et al. (1998) proposed a method for CRPs design based on the simplified propeller theory in order to optimize the pitch and thickness distributions of the propellers.

Paik et al. (2000) applied the panel method to predict the CRPs wake behavior. The outlet vortex structure was modeled by the wake model proposed by Greeley and Kerwin (1982), the obtained results were in agreement with their experimental results. Liu (2009) used the potential panel method to study the hydrodynamic interaction between the two propellers by introducing the mean values of the induced velocities. The results obtained showed that at high shaft frequencies, the panel method has no advantage compared to the lifting surface (LSD) method. The authors concluded that these results can be further improved by adjusting the wake model. Min et al. (2009) conducted a study on the design of full-scale contra-rotating propellers and deduced that the whole energy which contributes to the flow rotation can be recovered by the contra-rotating system if the system is well designed. Inukai (2011) carried out a study on CRPs characterized by the addition of a tip raked fins in order to increase the rear propeller diameter. He has shown that this configuration improves the efficiency by 1.5% compared to the conventional CRP without tip raked. Wang et al. (2012) have studied numerically the performance of two CRPs sets by testing different turbulence models and several time steps. They concluded that the SST $k-\omega$ turbulence model is suitable for the study of the flow around CRPs. They also recommended the use of a small-time step for CRPs with the same blade number of the two propellers and a relatively high time step for CRPs with different blade numbers. Xiong et al. (2016) conducted both numerical and experimental studies to explore the axial spacing effect on the hybrid CRPs pod hydrodynamic performance. They found that the increase in axial spacing generates a substantial reduction in the pod's thrust while the torque undergoes a slight variation, which results in a reduction of the global performances of the device. He et al. (2017) conducted a numerical study based on the sliding mesh technique to predict the performance of CRP in open water. They have shown that the CRPs thrust and torque are unsteady and periodic and that the vortex structure is very different from that produced by a single propeller. A comparison of performance results showed that CRPs efficiency is 2.2% higher than that of single propellers.

Feng et al. (2017) studied numerically the flow around the CRPs using the MRF (Multiple reference frame) techniques to analyze the variation of the thrust and torque propeller and the interaction between both propellers. They deduced that the forward propeller coefficients fluctuate more than those of the backward one. Paik (2017) performed numerical simulations on CRPs in open water and auto propulsion conditions to study the wake hydrodynamic behavior with and without a rudder. The results showed that although the rudder contributes to the increase in thrust and torque, it does not have a considerable effect on the wake field. Hou and Hu (2018) applied the potential panel method to determine the CRPs hydrodynamic performance and pressure distribution on the blade surface in the non-cavitating condition. The authors concluded that the pressure field fluctuations around the CRP are significantly lower than those of the single propeller upstream and downstream near the hub. Nouri et al. (2018) optimized the CRPs propellers using the genetic algorithm with the Kringin method to determine the optimal radial pitch and camber distributions for both front and rear propellers. Kaewkhiaw (2018) conducted a numerical study based on the solution of *RANS* equations. The study evaluated hydrodynamic performance for both propellers of two CRPs models in steady and unsteady conditions. The obtained results are in good agreement with the experimental measurements of Miller (1976).

Despite the abundant literature dedicated to the study of simple propellers in general and contra-rotating propellers in particular, few surveys either numerical or experimental have been devoted to investigating the axial and the angular displacement effects and also the blade twist angle of the rear propeller. In order to contribute the understanding of the effect of these parameters on the CRPs hydrodynamic performances, the a numerical study is proposed to investigate the turbulent unsteady flow behavior around a new configuration of contra-rotating propellers in open water. The propellers tested are four-bladed *DTMB* propeller, characterized essentially by the diameter, the advance coefficient, the axial spacing, the angular spacing and the blade twist angle of the propellers.

2. Geometrical Characteristics of the Propellers

The studied propellers are contra-rotating four-bladed *DTMB* characterized by a modified *NACA 66* ($a=0.8$), without skew and rake. The three-dimensional geometrical shape of the propellers is generated through a program developed in Fortran language based on Miller's (1976) data. Two configurations are designed: the single propeller and the contra-rotating propeller (CRP). The backward propeller diameter is reduced by 2% compared to the forward one and the spacing in the axial direction between both propellers is set at 14% of the front propeller diameter. The main geometrical characteristics of the studied propellers shown in Fig. 1 are summarized in Table 1.

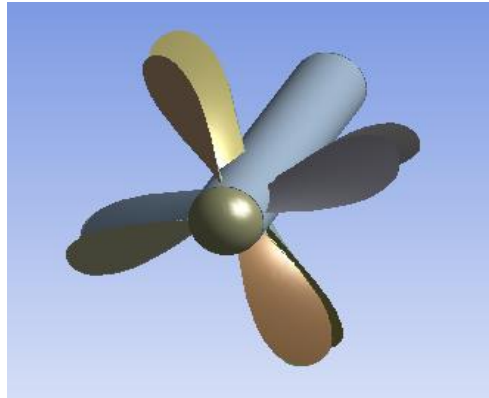


Fig. 1: Contra-rotating propeller (CRP)

Table 1: CRPs geometrical parameters

	Front	Rear
Propeller type	<i>DTMB3686</i>	<i>DTMB3687</i>
Diameter (m)	0.3052	0.2991
Pitch ratio at 0.7R	1.291	1.326
Expanded area ratio	0.303	0.324

3. Mathematical Model

3.1 Governing equations

The differential equations modeling the three-dimensional turbulent flow around propellers in the unsteady state express the principle of mass conservation and momentum. The fluid is considered Newtonian and incompressible, in a Cartesian reference frame these equations are written as follows:

$$\frac{\partial \rho}{\partial t} + \frac{\partial(\rho u_i)}{\partial x_i} = 0 \quad (1)$$

$$\frac{\partial(\rho u_i)}{\partial t} + \frac{\partial(\rho u_i u_j)}{\partial x_j} = -\frac{\partial P}{\partial x_i} + \frac{\partial}{\partial x_j} \left(\mu \frac{\partial u_i}{\partial x_j} - \rho u'_i u'_j \right) \quad (2)$$

The closure of the equation system is accomplished by the two-equation transport turbulence model $k-\omega$ SST where the mathematical formulation details can be easily consulted in Menter (1994).

3.2 Numerical procedure

In the open water CRPs test, the mean turbulent flow is reputed unsteady despite that the velocity inlet field is uniform. Physically, for one revolution the blade is subjected to periodic forces, but the entire propulsion system

produces stable forces in the time by compensation between the different blades. For CRPs operating in a uniform inflow, the geometric azimuth periodicity can be utilized (Dongya, 2017). Adopting periodic boundary conditions not only reduces the computation time but also can predict more accurately the open water performance of propeller using higher mesh density. The computational domain is reduced to a quarter from the physical domain to take into account the azimuthal periodicity condition. It is constituted by two blocks that are generated separately through the *Gambit* pre-processor and then connected using the *Fluent* solver. Fig. 2 illustrates the computation domain and the boundary conditions that are applied. The fluid domain rotates around the hub axis and the two juxtaposed blocks are linked by a rotating interface periodicity type. The inlet is located at $1.55D_F$ and the outlet is at $4.55D_F$ from the rear propeller. Their boundary conditions are uniform velocity and static pressure respectively. The computational domain is radially limited by a cylindrical envelope of diameter $3.28D_F$ as recommended by Kaewkhiaw (2018). The boundary condition applied to the outer wall is a symmetry condition. For the surfaces of the blades and hub, an adherence condition is imposed.

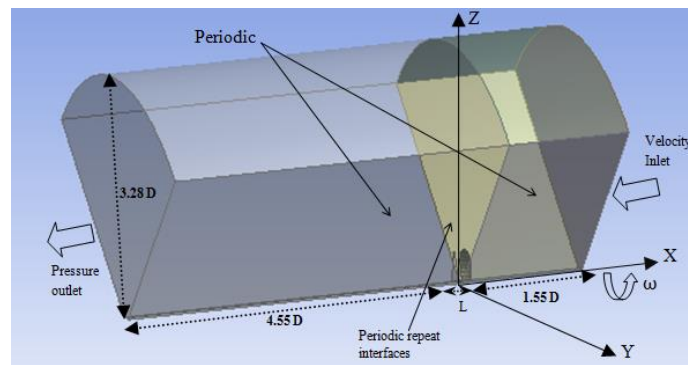


Fig. 2: Computational domain and boundary conditions

An unstructured mesh is generated using *Gambit* and *TGrid* due to the geometry complexity of the *DTMB* marine propellers. First, the blade surface is meshed by triangular elements using size function technique. The size of the elements is $0.0032 D_F$ in the regions near the leading and trailing edges and $0.022 D_F$ in the remaining part of the blade as shown in Fig. 3. Five prismatic cell layers with an expansion ratio of 1.1 are generated near the fixed and the moving solid walls by the *TGrid* code due to the high gradients. It has to be noted that the height of the first cell is estimated at $0.000001D_F$ corresponding to the recommended value of $y^+ < 1$ and that a sliding mesh is applied to the mobile interfaces connecting the two blocks. The cells number generated is about 1.3 million.

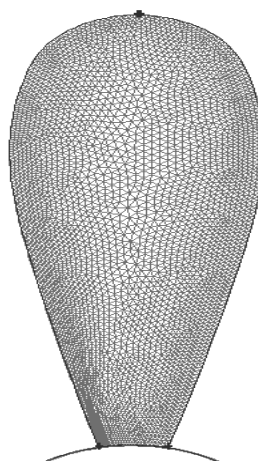


Fig. 3: Propeller blade surface grid.

The RANS averaged equations are solved numerically by the solver *Fluent*. The pressure-velocity coupling is of the *SIMPLEC* algorithm. The 2nd order upwind scheme is used for the discretization of convection terms while the standard scheme is chosen to discretize the continuity equation. The time step is set at 2.31410^{-4} seconds

corresponding to the rotation time of one degree of the propeller revolving at a speed of 720 rpm. The convergence of the calculations is controlled by following the evolution of the residues and the stability of the characteristic quantities representing the thrust and torque coefficients. The CPU execution time required to calculate the flow for each J was approximately 12 days on 8 parallel Intel Xeon processors with 3.5 GHz.

4. Results and Discussion

The behavior of the three-dimensional flow around the CRP is examined for different configurations by varying the axial spacing and relative angular positions between propellers and the twist angle of the backward propeller. For all numerical simulations, the advance coefficient J varies from 0.3 to 1.3. The obtained results are compared with those of single propellers operating in the same conditions.

The time-averaged thrust and torque coefficients for a period T are calculated as follows:

$$K_T = \frac{\int_0^T K'_T dt}{T} \quad (3)$$

$$K_Q = \frac{\int_0^T K'_Q dt}{T} \quad (4)$$

The analysis of propeller performance is essentially based on the following non-dimensional coefficients:

$$K_{TF} = \frac{T_F}{\rho n^2 D_F^4} \quad (5)$$

$$K_T = \frac{T_F + T_A}{\rho n^2 D_F^4} \quad (9)$$

$$K_{QF} = \frac{Q_F}{\rho n^2 D_F^5} \quad (6)$$

$$K_Q = \frac{Q_F + Q_A}{\rho n^2 D_F^5} \quad (10)$$

$$K_{TA} = \frac{T_A}{\rho n^2 D_F^4} \quad (7)$$

$$\eta_0 = \frac{J}{2\pi} \frac{K_T}{K_Q} \quad (11)$$

$$K_{QA} = \frac{Q_A}{\rho n^2 D_F^5} \quad (8)$$

where subscript F means front propeller and subscript A means rear propeller.

In order to validate the performed numerical simulations, the results for the CRP are compared with those of Miller (1976). Fig. 4 presents the front, rear and total propellers performances. The analysis of the figure shows that the thrust coefficient of the first propeller is in good agreement with the experiment, however the rear propeller thrust presents a slight difference which decreases with an increase of advance coefficient J . Concerning the torque coefficient, the difference is more significant for both propellers, this behavior is common to most studies using the RANS approach.

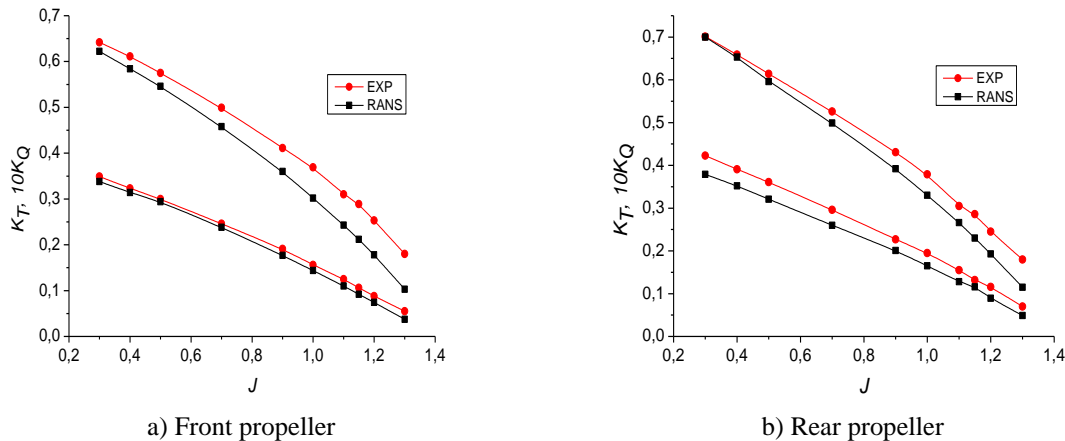
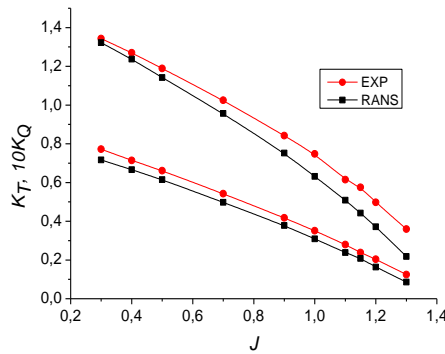


Fig. 4(a): CRPs hydrodynamic performances



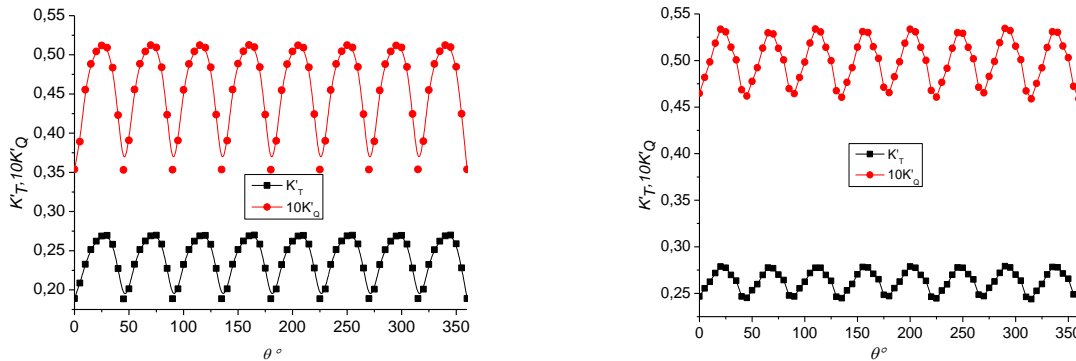
c) Total CRP

Fig. 4(b): CRPs hydrodynamic performances

Fig. 5 shows the thrust and torque distributions of the CRP propeller in terms of rotation angle. The analysis of the figure clearly shows the periodic behavior of the thrust and torque coefficients for a 45° angle, this behavior corresponds to the evolution of the thrust and torque CRP fluctuations given by the following formula:

$$f = f_n(m_F Z_F + m_A Z_A) \tag{12}$$

where f_n is the shaft frequency, $m_F Z_F = m_A Z_A$, Z_F and Z_A are the blades number of the front and rear propellers respectively, m_F and m_A are constants. If $Z_F = Z_A$, $m_F = m_A = 1$ and the frequencies of thrust and torque fluctuations are eight times of the propeller shaft frequency.



a) Front propeller

b) Rear propeller

Fig. 5: CRPs evolution of K_T and K_Q for one rotation, $J=1.15$

Table 2 quantifies the relative deviation of the thrust and torque coefficients for single and CRP propellers operating in the same conditions. The reference values are those of the single propeller. The advance coefficient is chosen as $J=1.15$ on the basis of the maximum propulsive efficiency. The comparison shows that although the thrust and the torque coefficients increase by 94% and 86% respectively, the CRP propeller efficiency is only about 4% higher than of the single propeller. This performance improvement is certainly due to the high rotational energy produced by the front propeller being entirely recovered by the rear propeller.

Table 2: Comparison of the CRPs performances with single propeller, $J=1.15$

	DTMB 3686 Front		DTMB 3687 Rear		Total			$\frac{K_T - K_{T \sin gle}}{K_{T \sin gle}}$	$\frac{K_Q - K_{Q \sin gle}}{K_{Q \sin gle}}$
	K_T	$10K_Q$	K_T	$10K_Q$	K_T	$10K_Q$	η		
Single	0.107	0.237	0.107	0.229	0.107	0.237	0.826	---	---
CRP	0.092	0.212	0.116	0.230	0.208	0.442	0.861	94%	86%

Fig. 6 illustrates the blade surface pressure distribution of the CRPs propeller for an advance coefficient $J=1.15$ and an axial spacing $L/D=0.14$. The obtained results show visibly that the core region of the suction side for both propellers is characterized by a high depression, while the pressure side has a large area of high pressure. Consequently, the contribution of the rear propeller in terms of total thrust is clearly confirmed.

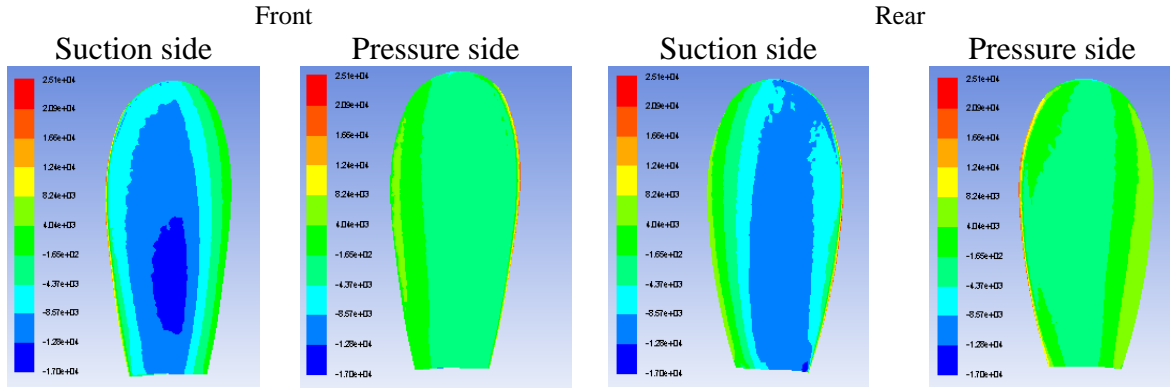


Fig. 6 : CRPs pressure distribution $L/D=0.14$, $J=1.15$

4.1 Diameter effect

Several numerical tests have been carried out to determine the equivalent single propeller diameter that develop the same thrust produced by CRPs for an advance coefficient equal to $J=1.15$. To achieve this purpose, two calculation processes can be used: - Run only one calculation for the single propeller to determine its thrust and then run several calculations for the CRP. The comparison of the two thrusts is done at each calculation step. - Run only one calculation for the CRP and several calculations for the single propeller. The second approach has been adopted in this work in order to reduce the CPU time. Indeed, the convergence of the computation for a single propeller requires approximately 6 hours while that of CRP requires approximately 12 days on 8 parallel Intel Xeon processors with 3.5 GHz. It should be noted that the CRP is characterized by a diameter of 0.3052 m and developed a thrust of 259.4 N. The equivalent single diameter is found about 0.3606 m, see Table 3. Indeed, a significant diameter gain around 15% is obtained.

Table 3: Diameter adjustment of single propeller for the same thrust of CRP.

Simulations	Single DTMB 3686 propeller for $J = 1.15$	
	D [m]	T [N]
01	0.5000	970.25
02	0.3805	321.66
03	0.3800	319.95
04	0.3700	287.45
05	0.3630	266.15
06	0.3615	261.87
07	0.3612	260.91
08	0.3611	260.52
09	0.3606	259.18

4.2 Axial displacement effect

Fig. 7 shows the evolution of K_T , K_Q and η as a function of J for different axial spacings L/D (0.14, 0.3, 0.4, 0.6 and 0.7). The analysis of the figure shows that the axial spacing effect on the CRPs propeller performance is negligible for this range. Indeed, all the tested configurations produce the same K_T and approximately a similar K_Q . With regard to the efficiency, the same statement is confirmed for the all advance coefficient less than 1.1, however, a slight efficiency improvement is predicted for $L/D= 0.14$ and $J=1.3$ compared to the remaining axial

spacing. It is probably due to the smallest gap between propellers that allows a high part recovery of energy by the backward propeller.

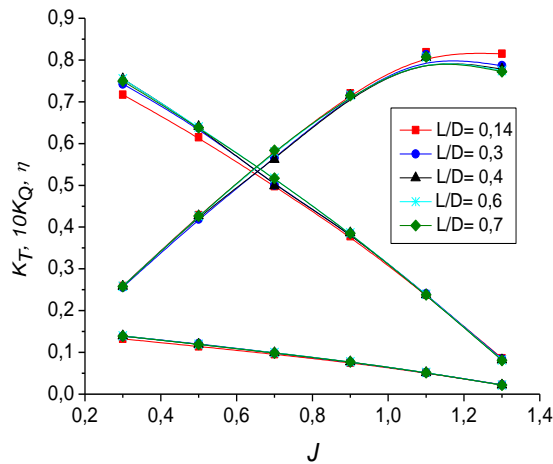


Fig. 7: CRPs hydrodynamic characteristics for different axial spacings.

Fig. 8 shows the velocity magnitude contours at the position A (middle position between the front and the rear propellers) and B (at the half axial displacement behind the rear propeller and the pressure on the suction and the pressure sides for both propellers blades for different axial spacing, $J=1.15$). The positions A and B are defined to the same distances; 21.59 mm from the front and rear propellers respectively. The analysis of the figure illustrates that for $L/D = 0.14$, the velocity field in plane A seems slightly more intense than that in plane B compared to the others studied spacings. The part of energy recovered by the backward propeller in this case can be explained by the hydrodynamic load applied to the rear propeller blades. The increase of the axial spacing decelerates the flow between the two propellers and induces a more or less pronounced uniformization of the flow over the two areas of the disc A and B.

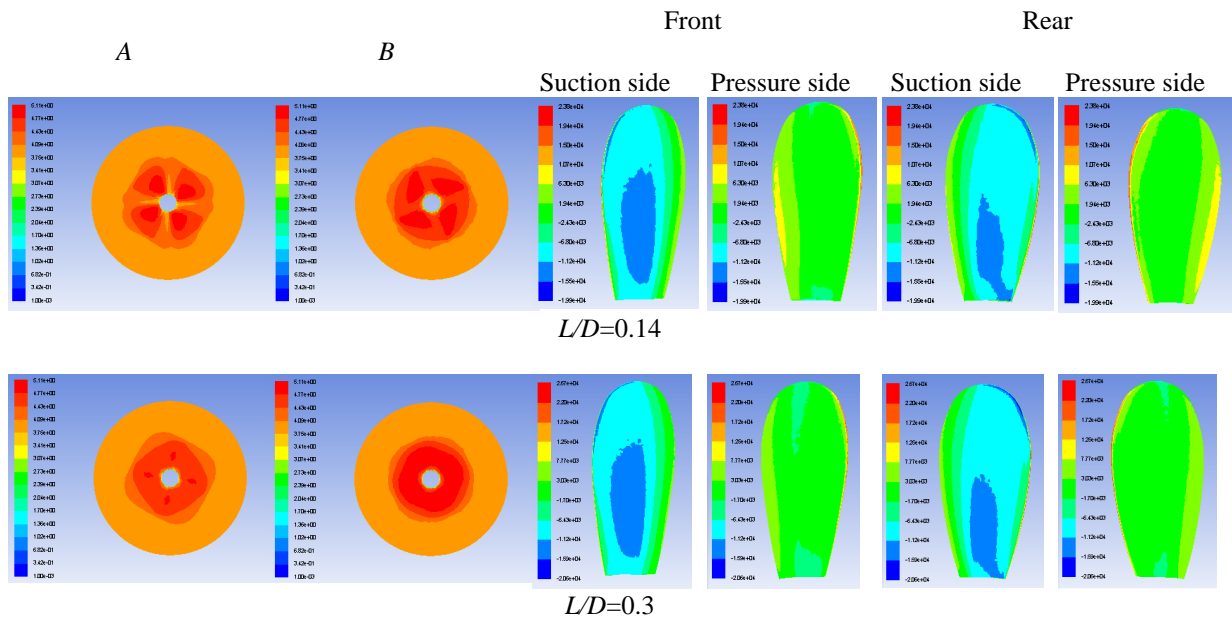


Fig. 8(a): Velocity magnitude contours at positions A and B and pressure distributions on both suction and pressure sides, $J=1.15$

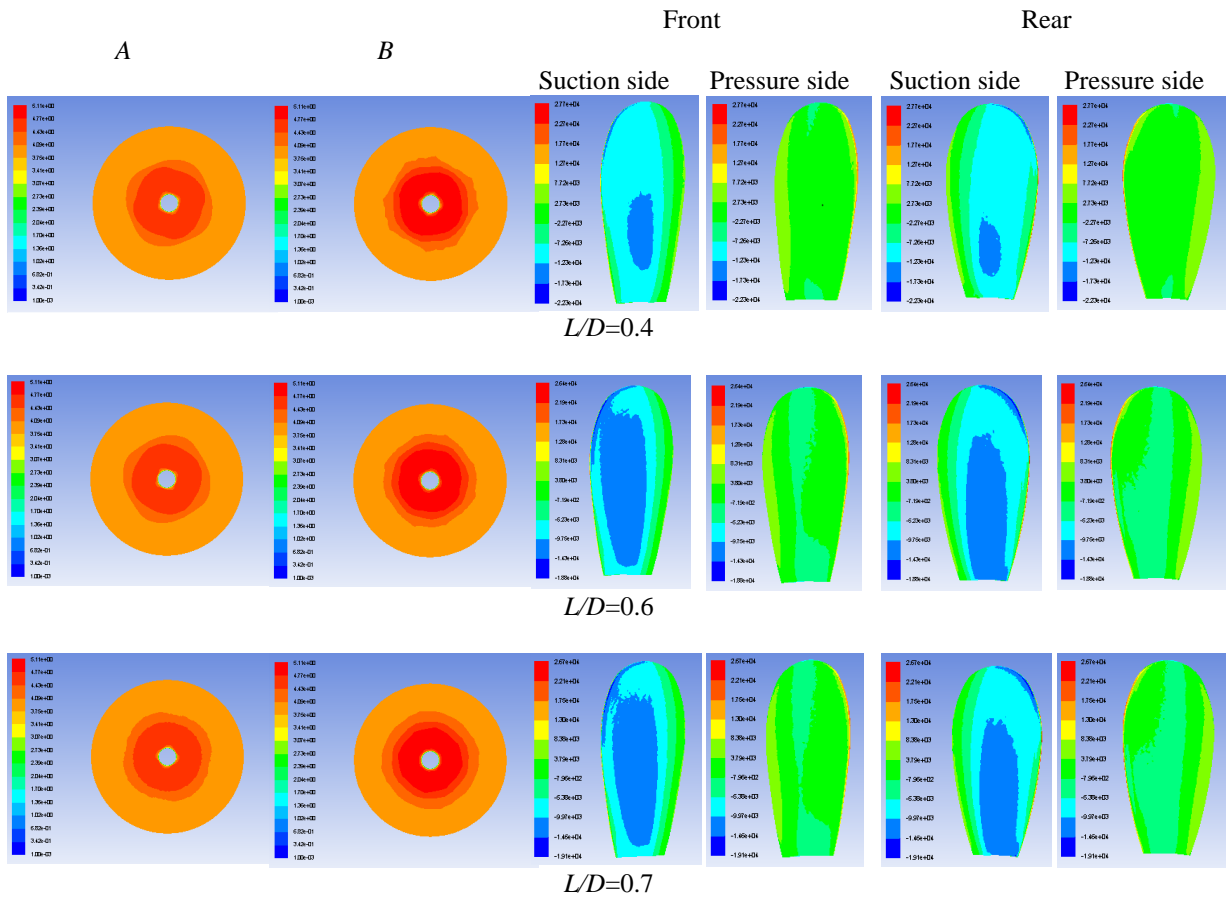


Fig. 8(b): Velocity magnitude contours at positions A and B and pressure distributions on both suction and pressure sides, $J=1.15$

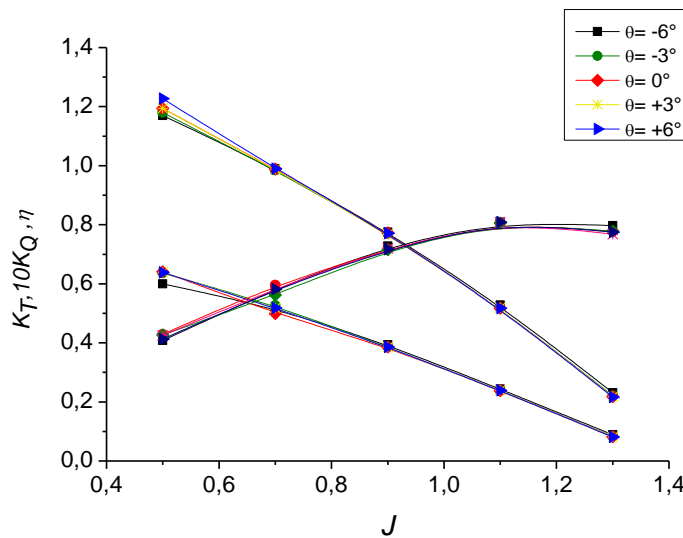


Fig. 9: CRPs hydrodynamic characteristics for different relative angular positions

4.3 Angular displacement effect

The optimal angular displacement (θ) of the rear propeller in regard to the front propeller can be defined as the one that allows the vortex of the front propeller to pass midway between the blades of the rear propeller. In

addition to the reference CRP propeller where the rear propeller is positioned exactly behind the front one $\theta=0^\circ$, four new CRP propeller configurations have been designed by varying the angular displacement with -6° , -3° , $+3^\circ$, $+6^\circ$. Fig. 9 shows the effect of relative angular position on the hydrodynamic characteristics of CRPs. In overall, all the tested configurations deliver the same thrust except the CRP with $\theta = -6^\circ$ for $J=0.5$ with a small decrease. While, the same torque is required for all configurations excepting the CRP with $\theta = +6^\circ$ for $J=0.5$ with a slight increase. Concerning the CRPs efficiency evolution, no obvious effect of angular displacement is observed for $J < 1.1$. The only and the outstanding difference which gives better efficiency is for the configuration with an angular displacement of $\theta = -6^\circ$ for $J=1.3$.

4.4 Twist angle effect

To provide necessary understanding of the twist angle effect, the flow behavior is examined by varying the twist angle (α) of the rear propeller from -5° to $+5^\circ$ over a range of J from 0.5 to 1.3. Fig. 10 shows the thrust, torque and efficiency coefficients of the CRP propellers as a function of the advance coefficient J with different twist angles of the rear propeller. The analysis of the results shows that the propeller with a twist angle of -3° gives the best thrust while the design with $\alpha = +5^\circ$ produces the lower thrust. The figure also illustrates that the torque coefficient increase with a decrease in the twist angle and the minimum value corresponds to configuration of $\alpha = +5^\circ$. The CRP configuration with $\alpha = -5$ represents the worst design due to its relatively high torque requirement and its low efficiency.

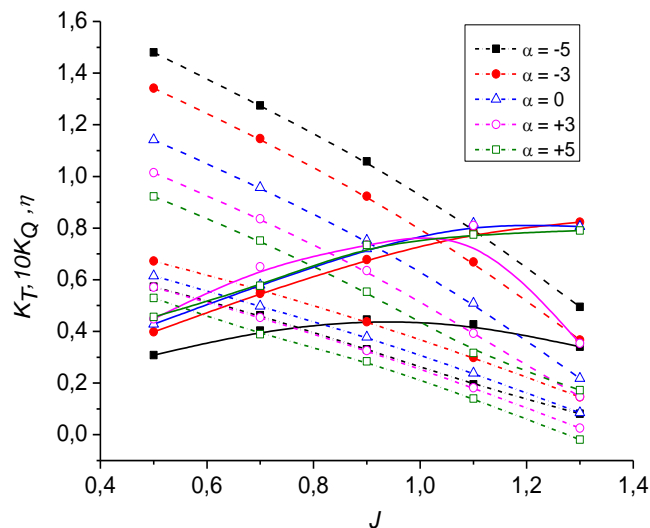


Fig. 10: Hydrodynamic characteristics for different twist angles.

Fig. 11 shows the velocity magnitude contours at the same position A and B defined previously and the pressure on the suction and the pressure sides for both propellers' blades for different twist angles, $J = 1.15$. The obtained results show that the velocity gradient at the area disc in position A is higher than that at the area disc in position B for all twist angles tested. The dynamic effect of this behavior is due to the fact that the energy transformation between the forward and backward propellers occurred in position A. The figure also shows that the flow is strongly decelerated near the wall. This deceleration is due to the friction forces induced by the boundary layer developed around the blades and which is characterized by a velocity decrease. For the twist angle $\theta = -3$, the results clearly show the presence of the trace of the marginal vortex released by each blade, this vortex is characterized by a velocity diminution at the core. Regarding the pressure contours on the blades, a significant depression is to be noted for positive twist angles. On the other hand, for negative twist angles, an increase of pressure is noted on the pressure side.

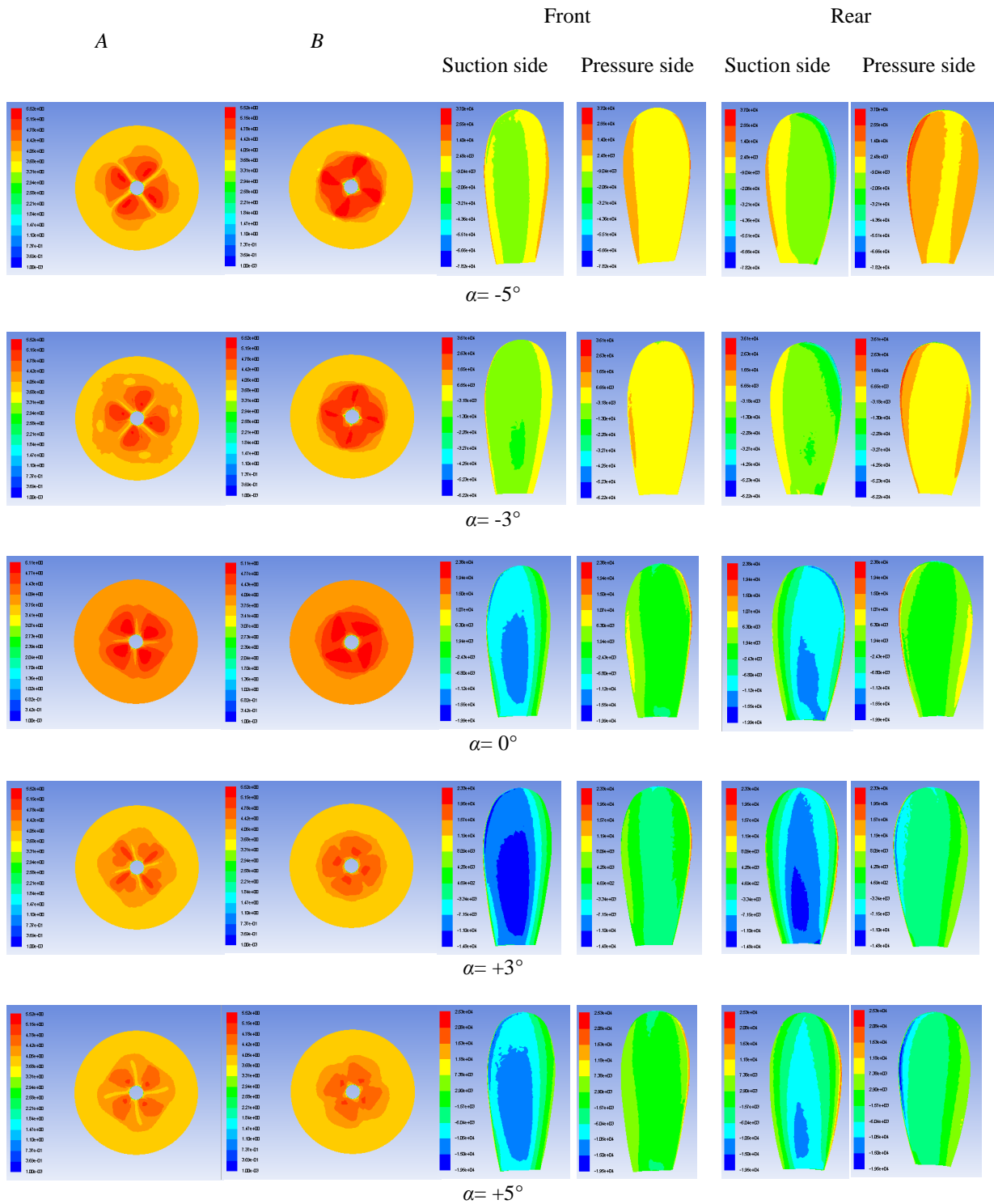


Fig. 11: Velocity magnitude contours at positions A and B and pressure distributions on both suction and pressure sides, $J=1.15$

5. Conclusion

CRPs contra-rotating *DTMB* type with four-bladed propellers are numerically studied and compared to single propeller operating in open water under similar conditions. The *RANS* equations are solved by the solver *Fluent* software. The following conclusions have been drawn:

- Although the thrust and the torque coefficients increase by 94% and 86% respectively, the CRPs propeller efficiency is only about 4% higher than that of the single propeller
- A significant diameter gains around 15% is obtained.
- For different axial displacements, all the tested configurations produce the same K_T and approximately a similar K_Q , and for the efficiency, the same statement is confirmed for the all advance coefficient less than 1.1.
- For the tested angular displacement, no obvious effect is observed for $J < 1.1$.
- The CRP configuration with $\alpha = -5$ represents the worst design and the propeller with a twist angle of -3° gives the best thrust.
- The results mentioned are convincing and can therefore contribute to the improvement of marine propellers. However, it remains that experimental tests are necessary to verify the results found.

Acknowledgements

The authors wish to thank "la direction générale de la recherche scientifique et du développement technologique DGRSDT" for their support and collaboration.

References

- Dongya H., Decheng W., Xinguo Y., (2017): Numerical Investigations of Open-water Performance of Contra-Rotating Propellers, Proceedings of the Twenty-seventh International Ocean and Polar Engineering Conference, ISBN 978-1-880653-97-5; ISSN 1098-6189.
- Feng, F., Geng, C., Guo, T., Huang, Q-Y. and Hu, J. (2017): Numerical simulation of contra rotating propellers, Proceedings of the International Conference on Manufacturing Engineering and Intelligent Materials Advances in Engineering, vol. 100, (ICMEIM).
- Greeley, D.S, and Kerwin, J.E. (1982): Numerical methods for propeller design and analysis in steady flow, SNAME transaction, Vol. 90, pp. 415-453
- He, D., Wan, D. and Yu, X. (2017): Numerical investigations of open-water performance of contra-rotating propellers, Proceedings of the 27th IOPEC, San Francisco, CA, USA, June 25-30.
- Hoshino, T. (1994): Experimental and theoretical analysis of propeller shaft forces of contra-rotating propellers and correlation with full scale data.
- Hou, L. X., and Hu, A. K. (2018): Spatial fluctuating pressure calculation of underwater counter rotating propellers under noncavitating condition. International Journal of Rotating Machinery, Vol. 2018. <https://doi.org/10.1155/2018/2909546>
- Inukai, Y. (2011): Development of contra-rotating propeller with tip-raked fins, 2nd International Symposium on Marine Propulsors SMP, Hamburg, Germany.
- Kaewkhiaw, P. (2018): CFD investigation on steady and unsteady performances of contra rotating propellers, Journal of Naval Architecture and Marine Engineering, Vol.15, No. 2, pp. 91-105. <http://dx.doi.org/10.3329/jname.v15i2.36225>
- Liu, X. L. (2009): A potential based panel method for prediction of steady and unsteady performances of contra-rotating propellers, Proceedings of the 1st International Symposium on Marine Propulsors, Trondheim, Norway. Yuiklm.
- Menter, F. R. (1994): Two-equation eddy-viscosity turbulence models for engineering applications, AIAA journal.32 Vol. 32, No. 8, pp. 1598-1605.
- Miller, M.L. (1976): Experimental determination of unsteady forces on contra-rotating propellers in uniform flow, David Taylor Naval Ship Research and Development Center, Report No. DTNSRDC/SPD-0659-01, Bethesda, Maryland, USA.
- Min, K. S., Chang, B. J., and Seo, H. W. (2009): Study on the contra-rotating propeller system design and full-scale performance prediction method, International Journal of Naval Architecture and Ocean Engineering, Vol. 1, No 1, pp. 29-38. <https://doi.org/10.2478/IJNAOE-2013-0004>
- Nouri, N. M., Mohammadi, S., and Zarezadeh, M. (2018): Optimization of a marine contra-rotating propellers set, Ocean Engineering. Vol. 167, pp. 397-404. <https://doi.org/10.1016/j.oceaneng.2018.05.067>
- Paik, K.J. (2017): Numerical study on the wake evolution of contra-rotating propeller in propeller open water and self-propulsion conditions. Brodogradnja, Shipbuilding, Vol. 68, pp.125-138 <http://dx.doi.org/10.21278/brod68108>

- Paik, K. J., Seo, S. B., and Chun, H. H. (2000): Analysis of contra-rotating propellers in steady flow by a vortex lattice method. *Journal of the Korean Society of Ocean Engineers*, Vol.14, No.2, pp.36-43.
- Sasaki, N., Murakami, M., Nozawa, K., Soejima, S., Shiraki, A., Aono, T., Fujimoto, T., Funeno, I., Ichii, N. and Onogi, H. (1998): Design system for optimum contra-rotating propellers, *Journal of marine science and technology*, Vol. 3, No. 1, pp. 3-21.
- Tsakonas, S., Jacobs, W. R., and Liao, P. (1983): Prediction of steady and unsteady loads and hydrodynamic forces on contra-rotating propellers, *Journal of Ship Research*, Vol. 27, No. 03, pp. 197-214.
- Wang, Z. Z., and Xiong, Y. (2012): Effect of time step size and turbulence model on the open water hydrodynamic performance prediction of contra-rotating propellers, *China Ocean Engineering*, Vol. 27, No. 2, pp. 193 – 204.
- Xiong, Y., Zhang, K., Wang, Z.Z. and Qi, W.J. (2016): Numerical and experimental studies on the effect of axial spacing on hydrodynamic performance of the hybrid CRP Pod propulsion system, *China Ocean Engineering*, Vol. 30, No. 4, pp. 627 – 636. <https://doi.org/10.1007/s13344-016-0040-8>
- Yang, C. J., and Tamashima, M. (1990): A simplified method to predict marine propeller performance including the effect of boss, *Transaction of the west Japan Society of Naval Architects*, No.80. pp, 23-33.
- Yang, C. J., Tamashima, M., Wang, G., & Yamazaki, R. (1991): Prediction of the steady performance of contra-rotating propellers by lifting surface theory, *Transactions of the West-Japan Society of Naval Architects*, Vol. 82, pp. 17-31.